

## Supporting Information

# Single Molecule Electrochemical Detection in Aqueous Solutions and Ionic Liquids

Joshua C. Byers, Binoy Paulose Nadappuram, David Perry, Kim McKelvey, Alex W.

Colburn, Patrick R. Unwin\*

Department of Chemistry, University of Warwick, Gibbet Hill Road, Coventry, CV4 7AL,  
U.K.

\*Corresponding author: [p.r.unwin@warwick.ac.uk](mailto:p.r.unwin@warwick.ac.uk)

<i>Index</i>	<i>Page</i>
<b>S1.</b> Experimental set-up	S2
<b>S2.</b> Piezo drift	S3
<b>S3.</b> Random walk simulation	S4
<b>S4.</b> Diffusion coefficient measurement	S7
<b>S5.</b> Electrode roughness	S8
References	S9

## S1. Experimental set-up

Micro-positioners (M-461, Newport) were used for initial positioning of the pipette in combination with a picomotor piezo linear actuator (New Focus). The picomotor (30 nm resolution) was used for coarse approach and the LISA linear actuator used for fine positioning of the pipette.

The working electrode currents,  $i_3$  and  $i_4$ , in Figure 1a of the main text were measured using two independent custom-built high sensitivity current-to-voltage converters. Initial current-to-voltage conversion took place in electrometer head units placed approximately 5 cm from the tip and substrate electrodes in order to minimize noise pick-up and input capacitance. The remote electrometer head units (each accurate to  $\pm 10\%$ ) were connected to auto-ranging gain/control units capable of switching automatically over four decade ranges from 1 fA/V to 1 pA/V. Each gain/control unit incorporated a variable first-order low-pass filter to control higher frequency noise. Further noise control was achieved using custom-built low-pass variable frequency eighth-order or sixteen-order brick wall filter units optimized for transient response and phase coherency. The time constants of the two filters were 100 ms and 50 ms.

## S2. Piezo drift

The drift of the  $z$ -piezo position was accurately determined by repeatedly approaching a silver wire towards a conductive diamond substrate and halting the approach as soon as a current was measured between the conductive diamond substrate and wire. The wire was then retracted by several micrometers (known precisely) above the substrate and the process was repeated every 10 minutes to observe the change in the approach distance as a function of time. The  $z$ -piezo position corresponds to the point where the wire makes contact with the substrate. Figure S1 shows that the  $z$ -piezo continuously drifted towards the substrate at a rate of approximately 10 nm per minute ( $0.17 \text{ nm s}^{-1}$ ), although this improved to less than 5 nm/min after > 3 h with the faraday cage closed. The drift was negligible on the timescale of typical measurements (a few seconds) and also much less than the slowest tip retract rate  $1.25 \text{ nm s}^{-1}$  (Fig. 3b main text) that was also used for some single molecule measurements.

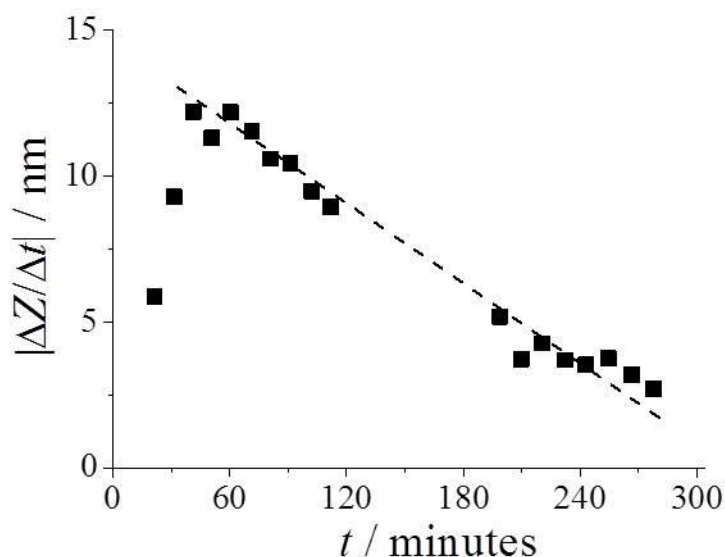


**Figure S1.** Thermal drift of  $z$ -piezo position as a function of time after closing the faraday cage. The dashed line is a guide for the eye.

### S3. Random walk simulation

A three dimensional (3D) random walk simulation was used to determine the position of a single molecule within the droplet (molecule trapped in the thin meniscus between the tip and surface). For the random walk simulation it was assumed that the molecule could move in the  $\pm x$ ,  $\pm y$ , or the  $\pm z$  direction with equal probability for each step. A reflecting boundary, defined by the pipette diameter, substrate surface, and probe end was used to constrain the position of the molecule within the droplet, such that if the molecule position attempted to exceed these dimensions it was reflected back from the boundary. A step size of  $dr = 4.05$  nm was used in the random walk simulation. This step is smaller than the tip-substrate separation (30 nm) for single molecule measurements and is significantly smaller than the diameter of an individual carbon microelectrode ( $\sim 1$   $\mu\text{m}$ ) or substrate ( $\sim 3$   $\mu\text{m}$ ) to allow adequate sampling of the nanogap geometry. The corresponding temporal step size was defined using  $dt = (dr)^2/2D$ , where  $D$  is the diffusion coefficient of  $\text{Ru}(\text{NH}_3)_6^{2/3+}$  ( $8.2 \times 10^{-6} \text{ cm}^2 \text{ s}^{-1}$ ), giving  $dt = 10$  ns. The temporal step size is 7 orders of magnitude smaller than the time constant of the electrometer (100 ms). Using these parameters, it was possible to accurately sample the 3D position of the molecule with sufficient spatial and temporal resolution over a reasonably long time period (1 s) for comparison with experimental data. Further parameters for the simulations are provided below in Table S1.

A charge transfer event occurred each time an oxidized (reduced) molecule collided with the reducing (oxidizing) electrode. The active area of each disk electrode was defined by the diameter of the carbon UME (1  $\mu\text{m}$ ) for the oxidizing electrode, and the total probe diameter (3  $\mu\text{m}$ ) for the reducing electrode. For each charge transfer event the associated current was calculated as  $i_{\text{redox}} = eD/z^2$ , where  $e$  is the charge of an electron, convolved with an instrument response function to generate the electrochemical current (Figure S2a). The following

expression was used to represent the instrument response,  $(2\pi/\tau) \cdot \exp(-2\pi/\tau)$ , where  $\tau$  is the time constant of the electrometer (100 ms) and  $t$  is time, and was found to be a reasonable approximation for the 100 ms rise time.<sup>2</sup> This led to transients (current-time profiles) such as that shown in Figure 4c of the main text. Figure S2 shows an example of the impact of the instrument response for an individual event (Figure S2a) and current transients (Figure S2b) obtained by convolving the occupancy plot with the electrometer response. It can be seen from Figure 3 of the main text and Figure S2b that the current magnitude and current-time course for a molecule trapped in the meniscus is similar to that seen experimentally.

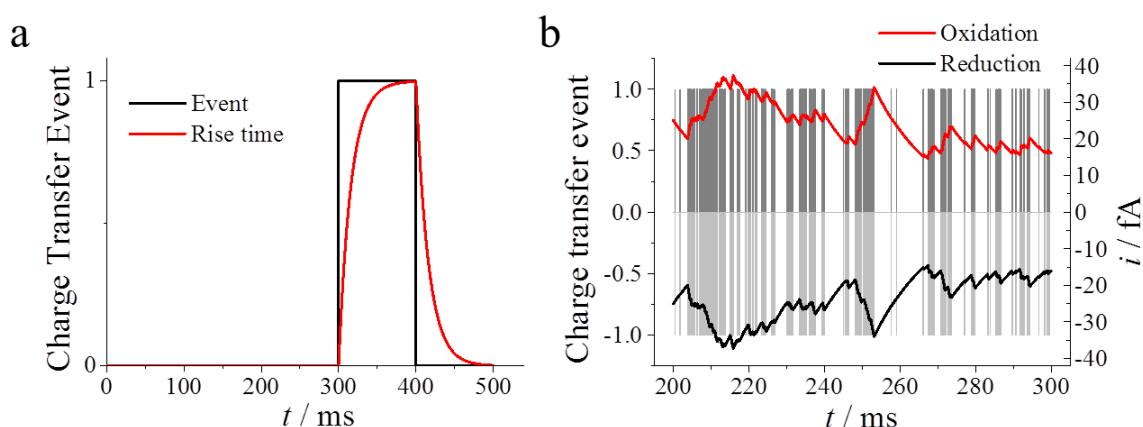


**Figure S2.** (a) Plot of charge transfer event (defined as 1 when an oxidized (reduced) molecule collides with the active area of the reducing (oxidizing) electrode, and zero otherwise) as a function of time (black line) and its convolution with the impulse function used to represent the rise time (100 ms) of electrometer (red line). (b) Charge transfer event (oxidation (dark gray) and reduction (light gray)) and corresponding electrochemical currents based on a 3D random walk.

**Table S1.** Random walk simulation parameters

Time step	10 ns
Diffusion coefficient	$8.2 \times 10^{-6} \text{ cm}^2 \text{ s}^{-1}$
Step size	4.05 nm
Probe radius	1.5 $\mu\text{m}$
Carbon UME radius	500 nm
Probe-substrate separation	30 nm
Electrometer time constant	100 ms
Sample time	10 $\mu\text{s}$
Samples per point	256
Molecule start position (x,y,z)	(0,0,15 nm)

#### S4. Diffusion Coefficient Measurement

The diffusion coefficient of  $\text{FcTMA}^+$  in the ionic liquid  $[\text{BMIM}][\text{BF}_4]$  was determined using linear sweep voltammetry and a Pt ultramicroelectrode in a bulk solution containing 50 mM of the redox mediator (ferrocenylmethyl)trimethylammonium ( $\text{FcTMA}^+$ ) hexafluorophosphate. A corresponding linear sweep voltammogram is shown in Figure S3 and the limiting current was used to determine the diffusion coefficient through the following expression for a disk ultramicroelectrode:<sup>3</sup>

$$i_{ss} = 4nFDCr \quad (1)$$

where  $i_{ss}$  is the limiting current,  $n$  ( $= 1$ ) is the number of electrons transferred,  $F$  is the Faraday constant,  $D$  is the diffusion coefficient,  $C$  (50 mM) is the bulk concentration of the redox mediator, and  $r$  (12.5  $\mu\text{m}$ ) is the radius of the ultramicroelectrode. For these conditions a diffusion coefficient of  $8.0 \times 10^{-12} \text{ m}^2 \text{ s}^{-1}$  was determined and is in line with recent values for a similar redox mediator (ferrocenemethanol) in  $[\text{BMIM}][\text{BF}_4]$  where a diffusion coefficient of  $1.3 \times 10^{-11} \text{ m}^2 \text{ s}^{-1}$  was reported.<sup>4</sup>

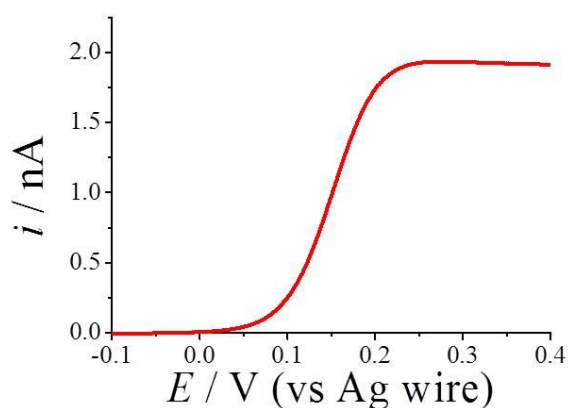


**Figure S3.** Linear sweep voltammogram of 50 mM  $\text{FcTMA}^+$  in the ionic liquid  $[\text{BMIM}][\text{BF}_4]$  using a 25  $\mu\text{m}$  diameter Pt UME and Ag wire QRCE.

## S5. Electrode Roughness

The working electrodes used in this work included a pyrolyzed carbon probe that was polished using a focused ion beam, a SPI-1 HOPG substrate, and a Pt coated glass slide. HOPG is an atomically flat electrode<sup>5</sup> and an atomic force microscope (AFM) image (Figure S4a) of a Pt coated glass slide showed an average surface roughness (RMS) of less than one nanometer. Very occasionally, a higher feature could be seen on the surface, but these were of low coverage compared to our micron-scale experiments and so would rarely be encountered. AFM measurements were carried out in tapping mode using a Bruker-Nano Enviroscope that was controlled using Nanoscope IV electronics.

Figure S4b shows a transmission electron microscope (TEM) (JEOL 2000FX) image of a pyrolyzed carbon electrode (side view). Both channels of a double barrelled quartz capillary were filled with carbon using the same procedure as for the quad probes. A smaller probe diameter with only two channels was used to allow for the acquisition of sufficiently high resolution TEM images. Figure S4b shows focused ion beam milling of the electrodes created extremely flat electrode surfaces without any noticeable surface features.

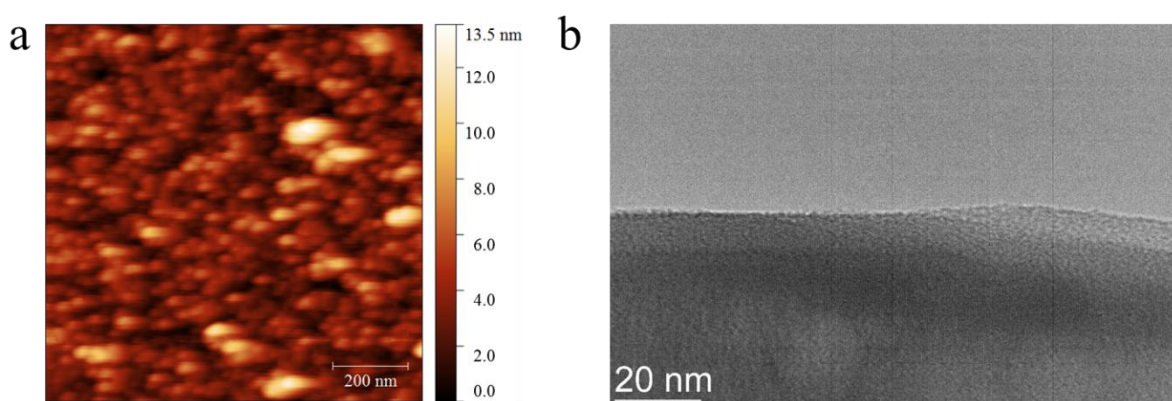


**Figure S4.** (a) Tapping-mode AFM image of a Pt-coated glass slide and (b) a TEM image (side view) of the surface of a carbon-filled quartz theta pipet.



## References

- (1) Ebejer, N.; Schnippering, M.; Colburn, A. W.; Edwards, M. A.; Unwin, P. R. *Anal. Chem.* **2010**, 82, 9141.
- (2) Singh, P. S.; Kätelhön, E.; Mathwig, K.; Wolfrum, B.; Lemay, S. G. *ACS Nano* **2012**, 6, 9662.
- (3) Bard, A. J.; Faulkner, L. R. *Electrochemical Methods: Fundamentals and Applications*, 2nd Edition.
- (4) Lovelock, K. R. J.; Ejigu, A.; Loh, S. F.; Men, S.; Licence, P.; Walsh, D. A. *Phys. Chem. Chem. Phys.* **2011**, 13, 10155.
- (5) Patel A.N.; Collignon, M.G.; O'Connell, M.A.; Hung, W.O.Y.; McKelvey, K.; Macpherson, J.V.; Unwin, P.R. *J. Am. Chem. Soc.* **2012**, 134, 20117.